


Adversarial Training for Graph Neural Networks via Graph Subspace Energy Optimization

Ganlin Liu , Ziling Liang , Xiaowei Huang , Xinping Yi , *Member, IEEE*, Shi Jin , *Fellow, IEEE*

Abstract—Despite impressive capability in learning over graph-structured data, graph neural networks (GNN) suffer from adversarial topology perturbation in both training and inference phases. While adversarial training has demonstrated remarkable effectiveness in image classification tasks, its suitability for GNN models has been doubted until a recent advance that shifts the focus from *transductive* to *inductive* learning. Still, GNN robustness in the inductive setting is under-explored, and it calls for deeper understanding of GNN adversarial training. To this end, we propose a new concept of graph subspace energy (GSE)—a generalization of graph energy that measures graph stability—of the adjacency matrix, as an indicator of GNN robustness against topology perturbations. To further demonstrate the effectiveness of such concept, we propose an adversarial training method with the perturbed graphs generated by maximizing the GSE regularization term, referred to as AT-GSE. To deal with the local and global topology perturbations raised respectively by LRBCD and PRBCD, we employ randomized SVD (RndSVD) and Nyström low-rank approximation to favor the different aspects of the GSE terms. An extensive set of experiments shows that AT-GSE outperforms consistently the state-of-the-art GNN adversarial training methods over different homophily and heterophily datasets in terms of adversarial accuracy, whilst more surprisingly achieving a superior clean accuracy on non-perturbed graphs.

Index Terms—Graph Neural Network, Adversarial Robustness, Graph Energy, Adversarial Training, Inductive Learning

I. INTRODUCTION

RECENT years have witnessed the remarkable effectiveness of graph neural networks (GNNs) in processing complex graph-structured data, such as social networks [1], physical systems [2], knowledge graphs [3], and many others (e.g., [4]). Graph convolution network (GCN) [5] is one of the pioneering GNN models that leverage only local information aggregation, yielding superior accuracy performance in node classification, graph classification, and link prediction tasks. Albeit promising in many tasks, it is noticed that GNN models are also vulnerable to adversarial attacks, such as label poisoning attacks (e.g., LafAK [6] and MGattack [7]) and graph topology poisoning and evasion attacks (e.g., Metattack [8], Nettetack [9], PRBCD [10] and LRBCD [11]). Such adversarial attacks could either mislead the training process to end up with a toxic GNN model (cf. poisoning attacks) or cause well-trained GNN models degraded performance in certain situations (cf. evasion attacks).

To defend against these adversarial attacks, there are an increasing number of studies that attempt to protect the GNN

model architectures or training process. For the graph poisoning attacks (e.g., Metattack and Nettetack), a number of robust GNN models, such as GCN-Jaccard [12], GCN-SVD [13], SimP-GCN [14] and Pro-GNN [15], have been proposed to preprocess the perturbed training graphs via graph properties, such as feature similarity, sparsity and low-rankness of adjacency matrix to improve the adversarial robustness. For graph evasion attacks (e.g., PRBCD and LRBCD), adversarial training (AT) has become a common method to improve GNN’s resistance against adversarial attacks without sacrificing classification accuracy as much as possible. Nevertheless, most adversarial training methods, such as Xu et al. [16], Xu et al. [17], Deng et al. [18], Feng et al. [19], Jin and Zhang [20], Chen et al. [21], Li et al. [22], and Guo et al. [23], are based on the transductive learning setting, which is impractical in real-world scenarios because it is unlikely the test set is informed in advance. A recent study [11] reveals both the theoretical and empirical limitations of adversarial training in the transductive learning setting, calling for rethinking adversarial training in a fully inductive learning setting, where test nodes are unavailable during training. This is the focus of the current work.

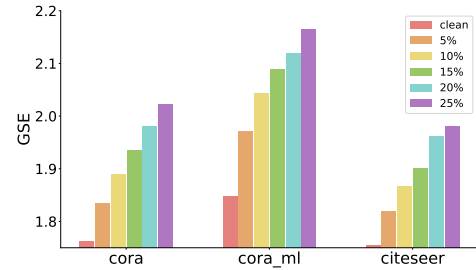


Fig. 1. Normalized graph subspace energy (GSE) of different datasets under adversarial topology attacks with different attack ratios.

In this paper, we take a look at graph topology evasion attacks from a graph energy perspective, and investigate adversarial training for GNN models in the fully inductive setting. In particular, given different graph datasets (e.g., Cora, Cora_ML, Citeseer) under Metattack, we observe, as shown in Figure 1, that the normalized graph energy exhibits certain property: the stronger the attack, the larger the graph subspace energy (GSE), a generalized concept of graph energy whose definition is in Definition 1. This suggests that graph energy could serve as a measurable indicator of graph topology attacks, through which we could be able to control the levels of graph topology attacks (such as Metattack). When it comes to adversarial training for graph neural networks, it would be possible to produce worst-case adversarial topology

G. Liu and X. Huang are with the Department of Computer Science, The University of Liverpool, Liverpool, UK. Email: {ganlin.liu, xiaowei.huang}@liverpool.ac.uk

Z. Liang, X. Yi, and S. Jin are with the National Mobile Communications Research Laboratory, Southeast University, Nanjing 210096, China. Email: {zliang, xyi, jinshi}@seu.edu.cn

perturbations by maximizing the corresponding graph energy, instead of resorting to gradient-based attacks as for the image classification tasks. Throughout the paper, we aim to show how graph energy can be employed in adversarial training and to what extent it can improve adversarial robustness of state-of-the-art GNN models. Specifically, our main *contributions* are summarized as follows:

- We propose a new concept of graph subspace energy (GSE), which can serve as a measurable indicator of GNN robustness against adversarial topology perturbation. The GSE is a generalization of graph energy, specifying graph energy contained in a subspace spanned by a set of singular vectors corresponding to a certain range of singular value distribution of the adjacency matrix. It is consistently observed adversarial topology attacks decrease node classification accuracy with the GSE increased simultaneously.
- Towards inductive learning of GNNs, we propose a novel adversarial training (AT) method with a minimax optimization formalism, referred to as AT-GSE, where the inner maximization aims to produce the worst-case graph perturbation with respect to the maximal GSE, and the outer minimization finds the model parameters over perturbed graphs via stochastic gradient descent (SGD) training. Notably, AT-GSE can be employed flexibly in various GNN models to improve adversarial robustness.
- To enhance AT-GSE against the local (e.g., LRBCD) and global (e.g., PRBCD) topology perturbations, we employ the randomized SVD (RndSVD) and Nyström low-rank approximation methods for the computations of the GSE terms, which place local and global emphases on graph spectrum, respectively. The former transforms the matrix into a smaller matrix that can be processed faster through randomization and QR decomposition, while the latter uses sampling and pseudo-inverse to obtain a low-rank approximation. They both increase efficiency and save storage space without sacrificing performance.

Through an extensive set of experiments, AT-GSE can improve the adversarial robustness of various datasets over the state-of-the-art GNN defending methods with a large margin. At the same time, GSE as a regularizer can consistently improve model clean accuracy across different GNN models. Also, RndSVD and Nyström methods have efficient and excellent performance in defending against local and global attacks respectively. An extensive set of experiments on 7 datasets containing both homophilic and heterophilic graphs demonstrate that our proposed AT-GSE has superior robustness, generalization, and scalability performance.

The rest of the paper is organized as follows. In Section II, we introduce the closely related work, including both adversarial attacks and defenses in the literature. Section III formally defines graph subspace energy and describes our proposed AT-GSE in detail. To reduce complexity, it also presents two methods: RndSVD and Nyström. In Section IV, experiments on 7 datasets are presented to compare our method with state-of-the-art ones with respect to both clean and adversarial accuracy. Finally, we conclude the paper in Section V.

II. BACKGROUND

Although powerful in node classification tasks, graph neural networks (GNNs) are vulnerable to graph topology adversarial attacks (Section II-A), which cause model performance degradation. To defend against such attacks, there exist various methods that resist adversarial attacks and improve model robustness (cf. adversarial defenses in Section II-B).

A. Adversarial Attacks

With respect to different targets of graph data, adversarial attacks on graphs can be categorized into label attacks, node attribute attacks and graph topology attacks. These attacks aim to exploit vulnerabilities of the GNN models to what extent the modified label/attribute/topology data could result in misclassification or incorrect predictions.

The goal of **label attacks**, such as LafAK [6] and MGattack [7], is mainly to mislead the model classification as much as possible by flipping a few target labels. In contrast, adversarial topology attacks pay more attention to modifying the graph structure. More specifically, adversarial topology attacks can be divided into poisoning and evasion attacks according to different stages when attacks happen. **Poisoning attacks** occur before training the model. There are two representative poisoning attacks: Metattack [8] treats the graph structure as a hyper-parameter to strategically modify the graph topology; Nettack [9] iteratively identifies which edge modifications will cause the largest degradation in model performance. It is worth noting that some poisoning attacks are also applicable to the inference phase as evasion attacks, where the latter is our focus.

Our focus in this paper is placed on **evasion attacks**, where the topology attack happens on well-trained GNN models in the inference phase. There are only a few graph evasion attacks in the literature, such as projected randomized block coordinate descent (PRBCD) [10] and locally constrained randomized block coordinate descent (LRBCD) [11]. The PRBCD attack is a gradient-based attack framework building upon a variant of the classic block coordinate descent (BCD) algorithm. In PRBCD, optimization variables are divided into blocks, with blocks of variables randomly selected to update on each iteration — such randomization helps convergence — followed by a projection step to ensure that the updated variables satisfy any constraints or bounds. As an extension of PRBCD, LRBCD adds local constraints that apply to specific subsets of variables rather than just the global objective function, yielding efficient attacks containing local constraints.

B. Adversarial Defenses

To protect graph neural networks from the adversarial attacks, different **robust models** have been proposed. GCN-Jaccard [12], SimP-GCN [14], and GCN-SVD [13] preprocess the adjacency matrix of the graph and use similarity or low-rank approximation to filter noise. Pro-GNN [15] adds some regularizers to the loss function to protect the low-rankness and sparsity of the graph properties. Robust-GCN [24] uses Gaussian distribution as the hidden representation in the convolutional layer to absorb the effects of adversarial attacks. This type of robust models resists poisoning attacks.

For evasion attacks, a preferred method is **adversarial training (AT)**. The main goal of AT is to enhance the robustness and generalization of a model by exposing it to adversarial examples during training. Many studies verify that it is effective in improving the classification accuracy on clean graphs and the robustness of machine learning against various adversarial attacks. At present, AT has many variants based on adversarial examples generated by different attacks, such as Xu et al. [16], Xu et al. [17], Deng et al. [18], Feng et al. [19], Jin and Zhang [20], Chen et al. [21], Li et al. [22], and Guo et al. [23]. The AT can be formulated as the following minimax optimization problem [11]

$$\arg \min_{\theta} \max_{\tilde{\mathcal{G}} \in \mathcal{B}(\mathcal{G})} \sum_{i=1}^n \ell(f_{\theta}(\tilde{\mathcal{G}})_i, y_i) \quad (1)$$

where the inner maximization is to generate a perturbed graph $\tilde{\mathcal{G}}$ from the graph set $\mathcal{B}(\mathcal{G})$ with certain budgets of perturbations that the given clean graph \mathcal{G} allows to generate, $f_{\theta}(\tilde{\mathcal{G}})_i$ is the prediction of node i based on the perturbed $\tilde{\mathcal{G}}$ with the model parameters θ , and ℓ is the loss of GNNs; the outer minimization consists of a normal GNN training process to find a robust model that produces correct label y_i with the perturbed graph $\tilde{\mathcal{G}}$. Usually, the perturbed graph set is defined as $\mathcal{B}(\mathcal{G}) \triangleq \{\tilde{\mathcal{G}} : \|A(\tilde{\mathcal{G}}) - A(\mathcal{G})\|_0 \leq \Delta\}$ where $A(\mathcal{G})$ is the adjacency matrix of \mathcal{G} , $\|A\|_0$ is the number of non-zero elements in the matrix A , and Δ specifies the budget of perturbed edges.

With respect to AT for GNNs, in the transductive learning setting, both labeled and unlabeled data are available during training such that the model can employ self-training to achieve perfect robustness without sacrificing accuracy. This, however, makes the majority of the previous studies that focus on the setting of transductive learning misleading due to theoretical and empirical limitations pointed out by Lukas et al. in [11]. Therefore, this paper investigates **adversarial training in a fully inductive setting**, following the argument in [11]. That is, in the inductive learning, the unlabeled data are completely unavailable during training, which is a more realistic scenario.

III. ADVERSARIAL TRAINING WITH GRAPH SUBSPACE ENERGY (AT-GSE)

In this section, we first introduce a new concept of graph subspace energy (GSE), followed by a novel adversarial training method with GSE being a regularization term. The GSE is used to produce worst-case perturbed graphs for adversarial training. To reduce time and space complexity, efficient GSE computation methods are also presented.

A. Graph Subspace Energy

Definition 1 (Graph Subspace Energy): For a graph \mathcal{G} with the adjacency matrix $A \in \mathbb{R}^{n \times n}$, the graph subspace energy is defined as

$$\text{GSE}(A, \beta_1, \beta_2) \triangleq \sum_{i=\lceil \beta_1 n \rceil}^{\lfloor \beta_2 n \rfloor} \sigma_i(A) \quad (2)$$

where $\beta_1 < \beta_2 \in [0, 1]$, n is the number of nodes in the graph \mathcal{G} , $\sigma_i(A)$ is the i -th largest singular value of A such that $\sigma_1(A) \geq \sigma_2(A) \geq \sigma_3(A) \geq \dots \geq \sigma_n(A) \geq 0$.

Graph subspace energy is a generalization of the well-established concept of graph energy, which is a measure of graph structural properties related to the rank and the number of edges. With the singular values and the corresponding singular vectors, graph energy provides information about the connected shape and clustering structure of the graph. From Definition 1, $\text{GSE}(A, \beta_1, \beta_2)$ measures the sum of singular values from k_1 to k_2 with $k_1 = \lfloor \beta_1 n \rfloor < k_2 = \lfloor \beta_2 n \rfloor$, which corresponds to a piece of singular value distribution of the adjacency matrix A . With the range (k_1, k_2) , $\text{GSE}(A, \beta_1, \beta_2)$ could be able to take a specific care of the subspace spanned by the singular vectors associated with $\{\sigma_i\}_{i=k_1+1}^{k_2}$. When $\beta_1 = 0$ and $\beta_2 = 1$, $\text{GSE}(A, 0, 1)$ reduces to nuclear norm.

The GSE can be simply computed by performing singular value decomposition (SVD) on a matrix, where a set of singular values and their associated singular vectors are obtained. The GSE can be regarded as a generalized truncated SVD, which reserves only a range of singular value distribution and their corresponding vectors. This truncation is commonly used for dimensionality reduction in various applications such as data compression, denoising, and low-rank approximation. It aims to preserve the essential information of the data in a lower dimensional subspace by retaining only the most important singular values. So, the truncation method is used to try to obtain the graph subspace energy by truncating the graph energy. We employ a more flexible truncation to freely retain the singular values according to the values of k_1 and k_2 . Figure 2 visualizes the changed GSE under LRBCD attacks with different attack ratios on Cora and Citeseer. Figure 2a and Figure 2c on the left are the curves formed by the singular values of the original and perturbed adjacency matrices. The areas under the curves between k_1 and k_2 can be interpreted as the GSE specified by β_1 and β_2 . The two right figures are GSE bar charts, each of which represents the GSE value at the corresponding attack ratio. It can be clearly seen that as the attack ratio increases, the GSE increases.

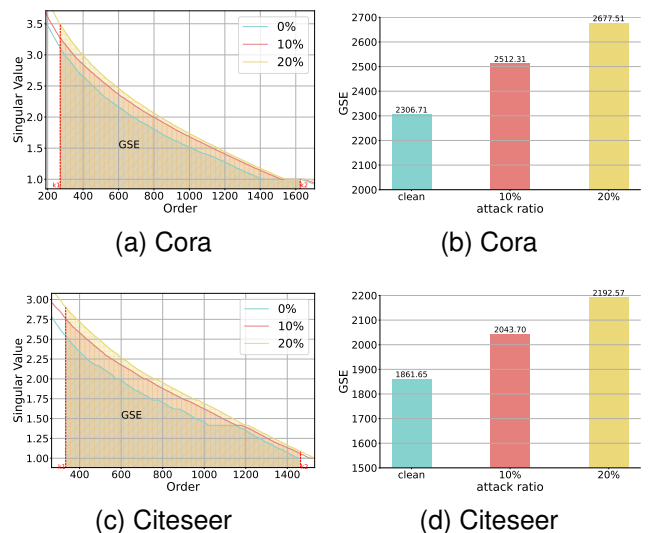


Fig. 2. A visual example of GSE under topology attacks of LRBCD with different attack ratios on Cora and Citeseer datasets.

B. Singular Value Distribution Shift under Topology Attacks

Adversarial training (AT) in GNNs is to improve the robustness and generalization capabilities of models against adversarial attacks or perturbations by exposing the learning model to adversarial examples during training. Following [11], we consider AT in a fully inductive learning. Adversarial examples are small perturbations injected into the input data on purpose in order to cause the model to misclassify the resulting perturbed data points. Searching for potential adversarial examples is usually an efficient way to identify the vulnerability of the trained models. By looking into the specific adversarial examples, it is hoped to find the possible underlying patterns.

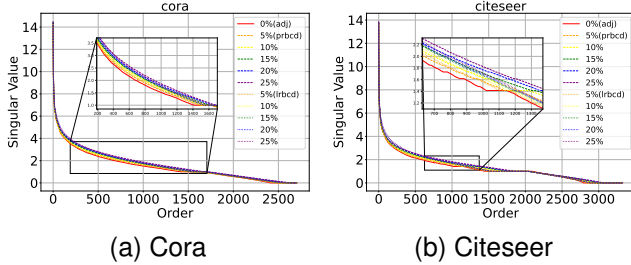


Fig. 3. The distribution shift of singular values of graph adjacency matrix under topology attacks of PRBCD and LRBCD with different attack ratios on Cora and Citeseer datasets.

Figure 3 showcases the singular value distribution shift of the adjacency matrices of the Cora and Citeseer datasets under different topology attacks (i.e., PRBCD and LRBCD), where there is a right-shift within a range of singular values. Therefore, the graph subspace energy (GSE) has the potential to have an influence on measuring the attack levels, i.e., the ratios of the number of perturbed edges to the total number of edges. Specifically, adversarial examples intend to change singular values of the adjacency matrices in a specific subspace.

C. GSE Offset Attacks and Adversarial Training

The above observation implies that adversarial topology attacks result in a potential right-shift of singular value distribution of the adjacency matrix, corresponding to an increase of the GSE of the associated graph. Inspired by this observation, in addition to the GNN adversarial training in Equation (1), the graph subspace energy term is added to the adversarial training as a regularizer to produce the adversarially perturbed graph. This framework is referred to as adversarial training with graph subspace energy (AT-GSE), whose minimax optimization problem can be formulated as

$$\arg \min_{\theta} \max_{\tilde{A} \in \mathcal{B}(A)} \left\{ \mathcal{L}_{GNN}(\theta, \tilde{A}, X, Y) + \gamma \text{GSE}(\tilde{A}, \beta_1, \beta_2) \right\} \quad (3)$$

where $\mathcal{B}(A) \triangleq \{\tilde{A} : \|A - \tilde{A}\|_0 \leq \Delta\}$ is the set of adjacency matrices of the perturbed graphs $\tilde{\mathcal{G}}$ with the number of perturbed edge budget being bounded by Δ , $\mathcal{L}_{GNN}(\theta, A, X, Y)$ is the expected/empirical loss of the GNN model with model parameter θ , adjacency matrix A , node attribute/feature set X and label set Y , GSE is the regularization term to help

produce perturbed graph \tilde{A} with maximized GSE, and γ is a predefined hyper-parameter to balance between the adversarial loss and the GSE regularization term.

The AT-GSE minimax optimization problem consists of an inner maximization problem to find a worst-case topology perturbation that increases the GNN loss function and the GSE term within the perturbed graph set, and an outer minimization is to obtain a robust GNN model to minimize the GNN loss given the perturbed graph. While the outer minimization can be solved alternatively by stochastic gradient descent, the inner maximization to find the worst-case perturbed graph is more challenging due to the gradient computation of the GSE term.

Regarding the inner maximization as to finding a GSE topology attack, we have two ways to generate the worst-case perturbed graph with adjacency matrix \tilde{A} . One simpler way is to randomly generate a number of perturbed graphs \tilde{A} within the graph set of $\mathcal{B}(A)$ in such a way that the perturbed graph with the maximum GSE is selected. This way of graph perturbation is referred to as ‘‘RndGSE’’ attack. On the other hand, given the above observation of singular value distribution shift, we introduce a GSE offset attack that aims to increase the singular values of the adjacency matrix A by simply adding a constant α to the singular values of interest, i.e.,

$$\text{GSE}_{\alpha}(A, \beta_1, \beta_2) = \sum_{i=k_1+1}^{k_2} (\sigma_i(A) + \alpha) \quad (4)$$

corresponding to a right-shift of singular value distribution, where α is a hyper-parameter fine-tuned with β_1 and β_2 . Given the perturbation budget $\|A - \tilde{A}\|_0 \leq \Delta$, we have a reference value of α . Let $\tilde{A} = A + E$ where $E \in \{0, 1\}^{n \times n}$ is the perturbation matrix such that $\|E\|_0 \leq \Delta$. According to the Hoffman-Wielandt inequality [25]

$$\sum_{k=1}^n (\sigma_k(A + E) - \sigma_k(A))^2 \leq \|E\|_F^2 \leq \Delta, \quad (5)$$

we can roughly set $n\alpha^2 \leq \Delta$ to ensure a reasonable adjustment, i.e., $\alpha \leq \sqrt{\frac{\Delta}{n}}$.

Therefore, the inner maximization can be done by gradient ascent of the GNN loss of the perturbed graph \tilde{A} , together with the additional gradient of the GSE regularizer. To obtain the gradient of GSE, we extend the proximal operator in [26] to the derivative of GSE offset. The projection follows the generation rules of GSE_{α} , increases the value of the truncated part of the singular values, and retains the largest singular value while discarding the smallest singular values, so as to produce the perturbed adjacency matrix. Specifically, the proximal operator on the GSE term can be written by

$$\text{prox}_{\alpha \|\cdot\|_{(k)}}(Z_k) = U_{k_2} \text{diag}(\sigma_1, \dots, \sigma_{k_1}, (\sigma_{k_1+1} + \alpha), \dots, (\sigma_{k_2} + \alpha)) V_{k_2}^T \quad (6)$$

where k is interpreted as $k_1 = \lfloor \beta_1 n \rfloor$ and $k_2 = \lfloor \beta_2 n \rfloor$, $0 \leq \beta_1 < \beta_2 \leq 1$, which are predefined parameters to represent the proportion, $Z = U \text{diag}(\sigma_1, \dots, \sigma_n) V^T$ is the singular value decomposition of Z , and U_{k_2}, V_{k_2} are the concatenated singular vectors associated with the singular values $\{\sigma_i\}_{i=1}^{k_2}$. It is worth noting that only the first k_2 -dimensional subspace is selected

to generate the perturbed graph and the last $k_2 - k_1$ singular values are adjusted with a constant α .

Algorithm 1: AT-GSE Algorithm

Input: Training/validation graph $\mathcal{G}_{t/v}$,
training/validation adjacency $A_{t/v}$,
training/validation labels $y_{t/v}$, GNN f_{θ_0} , epochs
 E , warm-up epochs W , loss ℓ , learning rate η ,
Hyper-parameters α, β_1, β_2

Output: GNN f_{θ^*}

```

1 Initialize  $\ell_{min} \leftarrow \infty$ 
2 for  $l = 1$  to  $W$  do
3    $\theta_l \leftarrow \theta_{l-1} + \eta \nabla_{\theta_{l-1}} (\ell(f_{\theta_{l-1}}(\hat{\mathcal{G}}_t), y_t))$ 
4 end
5 for  $l = W$  to  $E$  do
6   while stopping condition is not met do
7      $\tilde{A}_t \leftarrow \tilde{A}_t + \eta \nabla_{\tilde{A}_t} (\mathcal{L}_{GNN})$ 
8      $\tilde{A}_t \leftarrow \text{prox}_{\alpha \|\cdot\|_{(k)}} (\tilde{A}_t) \leftarrow \text{Equation (6)}$ 
9   end
10   $\hat{\mathcal{G}}_t \leftarrow \tilde{A}_t$ 
11   $\theta_l \leftarrow \theta_{l-1} + \eta \nabla_{\theta_{l-1}} (\ell(f_{\theta_{l-1}}(\hat{\mathcal{G}}_t), y_t))$ 
12  while stopping condition is not met do
13     $\tilde{A}_v \leftarrow \tilde{A}_v + \eta \nabla_{\tilde{A}_v} (\mathcal{L}_{GNN})$ 
14     $\tilde{A}_v \leftarrow \text{prox}_{\alpha \|\cdot\|_{(k)}} (\tilde{A}_v) \leftarrow \text{Equation (6)}$ 
15  end
16   $\hat{\mathcal{G}}_v \leftarrow \tilde{A}_v$ 
17  if  $\ell_{min} > \ell(f_{\theta_l}(\hat{\mathcal{G}}_v), y_v)$  then
18     $\ell_{min} \leftarrow \ell(f_{\theta_l}(\hat{\mathcal{G}}_v), y_v)$ 
19     $\theta^* \leftarrow \theta_l$ 
20  end
21 end
```

Using these updates and the projection rules, Algorithm 1 summarizes the details of our proposed AT-GSE method. Note that gradient ascent is employed to maximize the GNN loss function, and GSE offset, i.e., GSE_{α} , is used to enhance the graph subspace energy, both of which aim to produce perturbed graphs for outer minimization.

According to the proximal operator of Equation (6), we can clearly find that for GSE offset, how to effectively find the singular values and singular vectors of the adjacency matrix is the key point of the algorithm. The most common and original method is the SVD operation by, i.e., directly calculating the singular value matrix and the left and right singular value vector matrix of the adjacency matrix, and then performing related operations on them to get the final modified matrix.

D. Efficient GSE Computations

While directly employing SVD can get accurate singular values for our algorithm, the computational complexity of SVD is high, which may lead to a huge computing time for large-scale graph datasets. Moreover, for sparse graphs, directly applying SVD to adjacency matrices will produce three dense matrices, which may lead to a large increase in storage overhead. Therefore, although SVD has wide applicability in theory,

it may encounter some challenges in practical applications, especially when dealing with large-scale and sparse graphs. In order to handle large-scale and sparse graph datasets, we resort to the randomized singular value decomposition (RndSVD), and Nyström low-rank approximation methods.

1) *Randomized SVD (RndSVD)*: The core idea of RndSVD based AT-GSE is to generate adversarial examples that approximates the SVD of large matrices through random projection and dimensionality reduction techniques. This method is particularly suitable for processing very large and sparse matrices. It is roughly divided into three main steps: constructing a low-dimensional submatrix (line 8-14), calculating the SVD of the low-dimensional matrix (line 15-16), and constructing a perturbed adjacency matrix by the decomposed values. The detailed method is shown in Algorithm 2.

Algorithm 2: AT-GSE by RndSVD with Power Iteration

Input: Graph \mathcal{G} , adjacency A , labels y , GNN f_{θ_0} ,
epochs E , warm-up epochs W , loss ℓ , learning
rate η , Hyper-parameters α , $0 \leq \beta_1 < \beta_2 \leq 1$,
number of power iterations q

Output: GNN f_{θ^*}

```

1 Initialize  $\ell_{min} \leftarrow \infty$ , rank parameter  $k_1 = \lfloor \beta_1 n \rfloor$ ,  

 $k_2 = \lfloor \beta_2 n \rfloor$ 
2 for  $l = 1$  to  $W$  do
3    $\theta_l \leftarrow \theta_{l-1} + \eta \nabla_{\theta_{l-1}} (\ell(f_{\theta_{l-1}}(\hat{\mathcal{G}}), y))$ 
4 end
5 for  $l = W$  to  $E$  do
6   while stopping condition is not met do
7      $\tilde{A} \leftarrow \tilde{A} + \eta \nabla_{\tilde{A}} (\mathcal{L}_{GNN})$ 
8      $\Omega \in \mathbb{R}^{n \times (k_2+p)} \leftarrow \text{randn}(n, (k_2+p))$ 
9      $Y = \tilde{A}\Omega \in \mathbb{R}^{n \times (k_2+p)}$ 
10    for  $j = 1$  to  $q$  do
11       $Y \leftarrow \tilde{A}(\tilde{A}^T Y)$ 
12    end
13     $Q \in \mathbb{R}^{n \times (k_2+p)} \leftarrow \text{qr}(Y)$ 
14     $B \in \mathbb{R}^{(k_2+p) \times n} \leftarrow Q^T \tilde{A}$ 
15     $U_B, \Sigma, V \leftarrow \text{svd}(B)$ 
16     $U \leftarrow QU_B$ 
17     $\tilde{A} \leftarrow \text{prox}_{\alpha \|\cdot\|_{(k)}} (U, \Sigma, V) \leftarrow \text{Equation (6)}$ 
18  end
19   $\hat{\mathcal{G}} \leftarrow \tilde{A}$ 
20  if  $\ell_{min} > \ell(f_{\theta_l}(\hat{\mathcal{G}}), y)$  then
21     $\ell_{min} \leftarrow \ell(f_{\theta_l}(\hat{\mathcal{G}}), y)$ 
22     $\theta^* \leftarrow \theta_l$ 
23  end
24 end
```

The algorithm approximates the SVD of the matrix through random projection instead of exact calculation. Give a matrix A and a random tall matrix Ω , RndSVD computes the SVD on a low-dimensional matrix, which is the random projection of A onto the subspace spanned by the sampling matrix Ω . According to [27], the approximation error satisfies

$$\|A - \tilde{Q}\tilde{Q}^T A\| \leq \left[1 + 9\sqrt{k+p} \cdot \sqrt{n}\right] \sigma_{k+1} \quad (7)$$

with probability at least $1 - 3 \cdot p^{-p}$, where $\tilde{Q}\tilde{Q}^T$ is the subspace spanned by the random projection, k is the target rank, p is the oversampling parameter, $k + p \leq n$, and σ_{k+1} denotes the $(k + 1)$ -th largest singular values of A . When the oversampling $p = 5$, the failure probability of Equation (7) is $3 \cdot 5^{-5} = 0.00096$. That is a very small probability, indicating that the reliability of the approximate result is very high, thereby 5 is a reasonable assumption for oversampling.

In order to obtain a more accurate approximation result in randomized SVD, we combine the power iteration method to update Y , where the number of iterations is q , as shown in line 10-12 of Algorithm 2. Hence the expected approximate error bound [27] with q is written as

$$\mathbb{E}\|A - U\Sigma V^T\| \leq \left[1 + 4\sqrt{\frac{2n}{k-1}}\right]^{1/2q+1} \sigma_{k+1}. \quad (8)$$

Notably, as q increases, the error becomes smaller. That is, the more iterations there are, the smaller the approximation error is. Certainly, the more iterations, the longer the running time. So we also need to determine a reasonable value of q through the following time complexity.

RndSVD reduces computational complexity by compressing large matrices into smaller ones through random projection. The time complexity of RndSVD with power iteration is [27]

$$T_{RndSVD} = (2q + 2)kT_{mult} + O(2nk^2) \quad (9)$$

where T_{mult} is the flop count of a matrix-vector multiply with A . RndSVD is particularly suitable for large matrices that cannot be fully stored in memory. Only small matrices are calculated, which reduces memory usage. This is particularly important for processing large datasets, especially when the dataset is too large to be fully loaded into memory and the traditional SVD algorithm cannot be used. Equation (9) suggests that the time complexity is closely related to q . In practice, in order to ensure low time and space complexity, $q = 1$ or $q = 2$ is sufficient.

Overall, RndSVD provides an effective solution for large-scale datasets, which may sacrifice some accuracy in exchange for computational efficiency and memory usage efficiency. Although the traditional SVD algorithm can theoretically provide an accurate decomposition, it may encounter memory and computing time limitations on large graphs.

2) *Nyström Method*: The Nyström method reduces high time and space complexity by generating low-rank matrix approximations. It works as an information fusion method by using parts of the data multiple times to approximate the values we are interested in, such as the eigenvalues/eigenvectors of a matrix or the inverse of a matrix. Applying the Nyström method to machine learning problems can improve efficiency without significantly reducing performance.

Therefore, in order to further reduce the time complexity, we enhance AT-GSE with Nyström, by using it to find a low-rank approximation matrix, and then multiply it by a hyper-parameter α to generate a perturbed graph, thereby constructing an adversarial sample. The AT-GSE with Nyström method appears in Algorithm 3. Specifically, the Nyström method only needs to store and process a small part of the data W .

Algorithm 3: AT-GSE by Nyström Method

Input: Graph \mathcal{G} , adjacency A , labels y , GNN f_{θ_0} , epochs E , warm-up epochs W , loss ℓ , learning rate η , Hyper-parameters α , $0 \leq \beta \leq 1$

Output: GNN f_{θ^*}

```

1 Initialize  $\ell_{min} \leftarrow \infty$ , rank parameter  $k_2 = k = \lfloor \beta n \rfloor$ 
2 for  $l = 1$  to  $W$  do
3    $\theta_l \leftarrow \theta_{l-1} + \eta \nabla_{\theta_{l-1}} (\ell(f_{\theta_{l-1}}(\hat{\mathcal{G}}), y))$ 
4 end
5 for  $l = W$  to  $E$  do
6   while stopping condition is not met do
7      $\tilde{A}_t \leftarrow \tilde{A} + \eta \nabla_{\tilde{A}} (\mathcal{L}_{GNN})$ 
8      $c \leftarrow \text{randperm}(n)[:, k]$ 
9      $C \in \mathbb{R}^{n \times k} \leftarrow \tilde{A}[:, c]$ 
10     $W \in \mathbb{R}^{k \times k} \leftarrow C[c, :]$ 
11     $W^\dagger \leftarrow \text{pinv}(W)$ 
12     $\hat{A} \leftarrow CW^\dagger C^T$ 
13     $\tilde{A} \leftarrow \alpha \hat{A}$ 
14  end
15   $\hat{\mathcal{G}} \leftarrow \tilde{A}$ 
16  if  $\ell_{min} > \ell(f_{\theta_l}(\hat{\mathcal{G}}), y)$  then
17     $\ell_{min} \leftarrow \ell(f_{\theta_l}(\hat{\mathcal{G}}), y)$ 
18     $\theta^* \leftarrow \theta_l$ 
19  end
20 end

```

It generates a low-rank approximate matrix \hat{A} by using W many times, which can improve efficiency without significantly reducing performance.

The approximation error of the Nyström method under appropriate assumptions can be written [25]

$$\|A - CW^\dagger C^T\|_\xi \leq \|A - A_k\|_\xi + \epsilon \sum_{k=1}^n A_{ii}^2 \quad (10)$$

where $\xi = 2, F$, $\|\cdot\|_2$ and $\|\cdot\|_F$ denote the ℓ_2 and the Frobenius norm, respectively. And A_k is the best k -rank approximation of A , ϵ is an error parameter. Equation (10) shows that the error between the approximation matrix \hat{A} and the original matrix A will not exceed the error of the best k -rank approximation A_k plus an additional term with an adjustable parameter ϵ .

In conclusion, AT-GSE with the Nyström low-rank approximation focuses on the low-frequency band of graph spectrum, paying more attention to global topology changes. It is evident from Nyström's implementation steps that the largest k_2 singular values are adjusted. It is different from AT-GSE with RndSVD that preserves the low-frequency part corresponding to the largest $k_1 < k_2$ singular values whilst only adjusts the graph spectrum from k_1 to k_2 . Therefore, compared with AT-GSE with RndSVD emphasizes more on local topology changes, the Nyström method may pay more attention to global changes. Such differences make AT-GSE with RndSVD and Nyström method suitable respectively to defending against the local attacks (i.e., LRBCD) and the global attacks (i.e., PRBCD), as showcased in the experiments.

IV. EXPERIMENTS

Datasets. Cora, Cora_ML, Citeseer [28], and Pubmed [29] datasets are commonly used in the fields of graph semi-supervised learning for citation network analysis. All three datasets are citation networks, where nodes represent articles and edges represent citation relationships. These datasets are commonly used for tasks such as node classification and link prediction. The SBM (stochastic block model) [30] datasets are used in the field of network analysis and community detection. This dataset contains synthetic rather than real-world data, and the node features are Gaussian distributed. The adjacency matrices of SBM graphs exhibit a block structure, where nodes within the same block are more densely connected than those in different blocks. WikiCS is a graph dataset based on Wikipedia. The nodes correspond to Wikipedia papers in the field of computer science, and the edges are constructed based on the hyperlinks between papers. It also contains 10 categories representing different branches in the field of computer science. The statistics of these datasets are shown in Table I.

TABLE I
DATASET STATISTICS

Datasets	Homophily					Heterophily	
	Cora	Citeseer	Cora_ML	Pubmed	SBM	SBM	WikiCS
#Nodes	2708	2110	2810	19717	981	980	10311
#Edges	10556	7336	15962	44338	3890	3956	431108
#Features	1433	3703	2879	500	21	21	300
#Classes	7	6	7	3	2	2	10

Inductive Learning. Our focus is placed on inductive graph semi-supervised learning, where the validation and test nodes are not available during training so that merely memorizing the clean graphs does not lead to perfect robustness [11]. All experiments in Section IV follow a fully inductive semi-supervised setting as in [11].

Baselines. To evaluate the effectiveness of our proposed AT-GSE method on node classification, we compare it with some classical GNN models with and without adversarial training (AT). These baselines are briefly introduced as follows.

- **GCN [5]** is the cornerstone of most graph neural networks, but its lack of robustness makes it extremely vulnerable to adversarial attacks.
- **APPNP [31]** combines personalized propagation with neural prediction, where information from neighborhoods is propagated in a personalized way, giving more weight to nodes that are more relevant to the target nodes to achieve accurate and scalable predictions.
- **GPRGNN [32]:** generalized pagerank (GPR) can adaptively learn the weight of GPR, and then automatically adjust to the node label mode, thereby jointly optimizing the extraction of node features and topological information, ensuring that the model maintains excellent learning performance regardless of whether the node label is homophilic or heterophilic.
- **GNNs with AT [11]:** The above standard GNNs can be trained with adversarial training, by employing adversarial perturbations (e.g., LRBCD and PRBCD attacks) to generate adversarial examples for training data augmentation.

Setup. In the induction experiments of this paper, 20 nodes of each class were sampled as labeled training and validation sets. In addition, the test set consists of 10% of all nodes, and the remaining nodes are used as additional unlabeled nodes to be added to the training and validation sets. As mentioned in the baseline above, the comparison models in the following experiments include GCN, APPNP, GPRGNN, and these models with adversarial training. All experimental results are the mean accuracy and standard deviation obtained after running the model 10 times. Our method employs GCN, APPNP, and GPRGNN as the backbone GNN models to find the maximal loss function in the experiments. By adjusting the truncated singular values of the adjacency matrix, through modifying α and β in Equation (3), we obtain the maximized GSE term, thereby generating the expected robust model.

A. Hypothesis

Our experiments aim to verify the following hypotheses:

- 1). AT-GSE can improve over the natural training on existing GNN models with respect to the clean accuracy.
- 2). AT-GSE can improve adversarial robustness on different datasets, including homophilic and heterophilic graphs, improving over state-of-the-art methods.
- 3). Low-rank approximation methods (Nyström) are more suitable for defending against global attacks – PRBCD, while more specific spectrum adjustments (RndSVD) are more suitable against local attacks – LRBCD.

B. Robustness Performance

Our focus on robustness performance is placed on the ability of the GNN models to maintain accuracy against adversarial topology attacks, or perturbations, referred to as adversarial accuracy. To empirically verify the effectiveness of our proposed AT-GSE method, we evaluate the adversarial accuracy of the trained GNN models with different AT methods against topology perturbations on homophily and heterophily datasets under different ratios of perturbed edges. The following tables report the node classification results of AT-GSE and its related models, and some classic GNNs with and without adversarial training are included for comparison. From the results, we have the following observations.

1) Models with adversarial training generally achieve better adversarial robustness than their original models. Table II shows that adversarial training based on multiple backbone models has a certain defensive effect against various attacks. Specifically, adversarial training helps improve the defense capabilities of GNNs against malicious attacks and adversarial threats. By training the network to withstand adversarial examples, the impact of small budgets on the input data can be mitigated, thereby improving the reliability of the network.

2) Adversarial training with simple data augmentation could also yield effective robust models. Figure 3 shows that the singular value distribution of the perturbed graphs exhibits a right-shift. In adversarial training, adversarial examples can be randomly generated with the one having the largest GSE is selected as the worst-case perturbed graph for further training.

TABLE II

COMPARISON BETWEEN AT-GSE AND BASELINES UNDER VARIOUS ATTACKS ON CITESEER WITHOUT SELF-TRAINING. THE FIRST COLUMN (ATTACK), SECOND COLUMN (MODEL) AND THIRD COLUMN (AT, × MEANS MODELS WITHOUT AT) SHOW THE NAMES OF THE ATTACKS, BASELINE MODELS, AND OUR PROPOSED METHODS (AT-GSE) TOGETHER. APPNP AND GPRGNN REPRESENT THE BACKBONE GNN MODEL. THE PERCENTAGE (0%, 10%, AND 25%) IS THE RATE OF BUDGET. THE BEST RESULT IS HIGHLIGHTED IN BOLD.

Attack	Model	AT	0%	10%	25%
LRBCD	APPNP	×	70.93±0.88	62.24±1.18	56.03±1.58
		LRBCD	71.96±0.00	63.04±0.82	57.76±1.70
		AT-GSE	73.97±0.30	68.46±1.28	65.23±0.94
	GPRGNN	×	59.63±0.84	54.07±0.91	45.05±1.19
		LRBCD	59.35±0.00	56.45±0.65	53.79±1.15
		AT-GSE	72.90±0.00	71.45±0.25	67.85±0.72
PRBCD	APPNP	×	70.75±1.29	59.58±1.33	50.84±1.49
		LRBCD	73.55±0.56	62.52±0.50	54.35±0.91
		AT-GSE	73.22±0.51	65.75±0.81	60.05±0.64
	GPRGNN	×	60.28±2.80	53.46±1.76	47.38±1.39
		LRBCD	58.97±5.67	55.79±2.79	53.18±1.60
		AT-GSE	71.64±1.18	69.67±0.64	68.50±1.05
PGD	APPNP	×	69.72±1.12	63.46±1.28	55.65±0.53
		LRBCD	71.68±0.84	63.22±0.98	57.52±1.26
		AT-GSE	73.46±0.65	67.76±1.02	62.85±0.82
	GPRGNN	×	63.55±1.14	56.92±0.69	52.24±1.83
		LRBCD	62.34±1.50	60.00±1.50	56.92±0.19
		AT-GSE	74.25±0.92	71.96±0.72	68.83±0.21

This is referred to as *RndGSE*, a data augmentation method for adversarial training. According to Table III and Table IV, i.e., the row where the model corresponds to *RndGSE*, we observe that adversarial training with *RndGSE* can yield robust GNN models with comparable adversarial accuracy performance, although it is inferior to AT-GSE. This is evident that GSE can be an effective indicator of GNN robustness.

3) AT-GSE is effective against various adversarial attacks. After random GSE (*RndGSE*) showed its excellent robustness, we refined the range of hyper-parameters in GSE and proposed the AT-GSE model. Table II summarizes the robustness performance of AT-GSE when facing attacks on LRBCD, PRBCD, or PGD with APPNP and GPRGNN as the backbone models. As can be seen from the table, AT-GSE shows excellent robustness under various attacks, that is, it helps to resist a variety of adversarial attacks.

4) AT-GSE is an effective defense method to improve GNN adversarial robustness. The essential difference between AT-GSE and the existing ones is the way to generate adversarially perturbed graphs for inductive learning. *AT-GSE* as a *gradient-based* method attempts to generate perturbations by adjusting the singular value distribution of the adjacency matrix of the clean graph, so that the adversarial training on such perturbed graph could track the structural properties of the underlying graph. As is evident from the results in Table III, Table IV, Table V, and Table VI, we compare the empirical robustness of our proposed model with GCN, APPNP, and GPRGNN with and without adversarial training on Cora, Citeseer, Cora_ML and SBM (homo.). The best accuracy is shown in bold in the tables, which clearly shows that our proposed AT-GSE outperforms other baselines in terms of robustness. In these experimental results, we observed that

our proposed *AT-GSE* method outperforms other baselines in most cases. All these tables show that under both LRBCD and PRBCD attacks, AT-GSE significantly improves the robustness of standard GNNs. Given that this method maintains the best accuracy even on clean data sets, i.e., unperturbed graphs, it is reasonable to verify that AT-GSE greatly improves the robustness of GNN while still maintaining the accuracy of classification.

5) AT-GSE is selective with different GNN models to maintain its clean and adversarial accuracy on various datasets. Our proposed AT-GSE algorithm works together with different GNN models, where different models could yield distinct performance. The previous columns of AT-GSE in Table V and Table VI are marked with the benchmark GNN models, upon which the robust models are adversarially trained. Specifically, for the Cora_ML dataset, GPRGNN and APPNP models with AT-GSE are more suitable to defend against PRBCD and LRBCD attacks, respectively, and for SBM (homo.), GCN with AT-GSE is the best choice.

6) AT-GSE can also achieve good prediction results on heterophily graphs. Table VII presents the performance of AT-GSE and baselines on a heterophily graph. It appears our proposed AT-GSE method significantly improves the robustness against adversarial attacks and the accuracy of clean datasets with a large margin. Remarkably, the adversarially trained GPRGNN model with AT-GSE achieves state-of-the-art performance on the clean SBM dataset.

7) GNN models with AT-GSE can not only improve adversarial robustness but also help generalization ability. Table III shows that our proposed AT-GSE method still has stronger prediction performance on clean graphs, even though the models are adversarially trained. It can be concluded that AT-GSE not only improves adversarial accuracy but also enhances clean accuracy. To further certify the generalization ability of the AT-GSE model, we specifically tested the accuracy of backbone models (GCN, APPNP, and GPRGNN) with and without AT-GSE on different 5 clean graphs, as shown in Table VIII. It can be seen that the performance of AT-GSE based on the three models of GCN, APPNP, and GPRGNN is better than the original normally-trained ones. As such, we conclude that AT-GSE has strong generalization ability as it can be employed by any backbone model, and its superiority to the original model shows that it can improve the classification accuracy of the model on clean graphs.

To sum up, based on the experimental results of the naturally and adversarially trained GNN models on various graph datasets, we conclude that AT-GSE consistently improves adversarial robustness and clean accuracy not only on homophilic datasets but also on heterophilic graphs. Therefore, AT-GSE can be widely employed to train robust and generalizable GNN models to mine different types of graph-structured data.

C. Scalability Performance

Speaking of scalability performance, it is necessary to consider aspects such as *computing efficiency, data size, storage overhead, and prediction accuracy*.

Based on the above experiments, we can conclude that AT-GSE has excellent robustness and generalization and is

TABLE III

COMPARISON BETWEEN AT-GSE AND BASELINES ON CORA. THE FIRST COLUMN (MODEL) AND THE SECOND COLUMN (AT, × MEANS MODELS WITHOUT AT) SHOW THE NAMES OF THE BASELINES AND OUR PROPOSED METHODS (LIGHT GRAY BACKGROUND) TOGETHER. GPRGNN IN THE LAST LINE REPRESENTS THE BACKBONE GNN MODEL FOR AT-GSE. THE SECOND LINE IS THE ATTACK RATIO. THE BEST RESULT IS HIGHLIGHTED IN **BOLD**.

Model	AT	Clean	LRBCD	PRBCD	LRBCD	PRBCD	LRBCD	PRBCD
		0%	5%		10%		25%	
GCN	×	77.91±0.17	74.91±1.13	70.48±0.57	68.83±0.92	66.01±0.83	59.85±0.96	56.12±1.26
APPNP	×	79.05±1.06	74.95±0.72	72.34±1.66	69.63±0.62	69.27±0.68	63.66±0.78	60.00±0.86
GPRGNN	×	80.40±2.11	77.88±1.91	74.80±1.14	74.73±1.21	71.50±1.55	65.86±1.11	65.60±0.62
GCN	LRBCD	77.73±0.27	73.92±1.12	71.17±0.52	69.60±0.94	67.47±0.91	62.31±1.09	59.93±0.72
	PRBCD	80.15±0.15	75.42±0.96	73.59±0.45	69.85±0.79	69.41±0.44	62.31±0.95	60.48±0.64
APPNP	LRBCD	80.81±0.29	76.48±0.71	74.95±0.41	71.54±1.04	71.14±0.67	64.07±0.79	63.74±1.06
	PRBCD	81.72±0.38	76.59±1.08	73.77±0.52	70.88±1.61	69.38±0.64	62.09±0.62	63.52±0.74
GPRGNN	LRBCD	81.32±0.57	78.72±0.83	76.96±1.94	72.89±0.46	74.62±1.51	69.56±1.45	67.55±0.87
	PRBCD	80.99±0.50	80.07±1.70	77.03±0.77	78.10±1.18	73.92±0.56	67.69±1.41	63.08±2.69
GPRGNN	RndGSE	80.84±0.33	79.82±0.20	77.47±0.38	77.51±0.60	74.58±0.66	73.30±0.60	70.33±0.66
GPRGNN	GSE	83.41±0.43	81.90±1.06	78.72±0.60	78.86±1.01	77.00±0.36	73.41±0.90	72.45±1.58
	RndSVD	85.42±0.22	83.92±0.35	79.01±0.61	82.34±0.27	75.57±0.43	73.59±0.60	73.48±0.52
	Nyström	84.69±0.59	81.43±0.40	81.39±0.39	79.89±0.60	80.00±0.52	73.15±1.57	76.26±1.82

TABLE IV

COMPARISON BETWEEN AT-GSE AND BASELINES ON CITESEER. THE FIRST COLUMN (MODEL) AND THE SECOND COLUMN (AT, × MEANS MODELS WITHOUT AT) SHOW THE NAMES OF THE BASELINES AND OUR PROPOSED METHODS (LIGHT GRAY BACKGROUND) TOGETHER. GPRGNN IN THE LAST LINE REPRESENTS THE BACKBONE GNN MODEL FOR AT-GSE. THE SECOND LINE IS THE RATE OF BUDGET. THE BEST RESULT IS HIGHLIGHTED IN **BOLD**.

Model	AT	Clean	LRBCD	PRBCD	LRBCD	PRBCD	LRBCD	PRBCD
		0%	5%		10%		25%	
GCN	×	71.73±0.48	66.40±1.03	64.25±1.05	63.46±0.78	59.07±1.07	53.74±1.35	48.18±0.74
APPNP	×	70.98±1.30	65.61±0.92	64.91±1.09	64.25±0.73	62.80±1.24	56.87±1.98	56.26±1.82
GPRGNN	×	74.44±0.30	65.33±0.69	69.86±0.76	63.97±0.57	66.21±0.81	58.13±0.94	61.21±0.78
GCN	LRBCD	74.35±0.44	73.22±1.20	69.58±0.61	71.17±0.91	65.89±0.89	67.57±0.76	59.53±0.89
	PRBCD	74.30±0.72	71.36±0.63	70.33±0.84	69.53±0.83	65.37±1.26	64.91±1.01	55.84±1.70
APPNP	LRBCD	73.83±0.00	72.38±0.33	70.93±0.28	69.72±0.35	68.46±0.31	65.89±0.63	64.77±1.22
	PRBCD	73.79±0.33	71.73±0.31	69.07±0.54	68.74±0.64	65.61±0.48	63.18±1.27	59.53±0.98
GPRGNN	LRBCD	74.35±1.54	72.99±1.04	71.07±1.31	68.79±0.78	67.76±0.78	65.42±0.84	62.90±0.67
	PRBCD	73.55±0.37	72.15±0.37	68.97±0.31	68.50±0.43	66.07±0.76	65.98±0.54	60.93±0.76
GPRGNN	RndGSE	75.14±0.46	68.32±0.19	73.74±0.65	67.85±0.50	72.71±0.37	65.09±0.55	71.59±0.50
GPRGNN	GSE	76.54±0.75	74.77±0.00	73.69±0.75	74.49±0.76	72.80±0.65	70.33±0.48	68.13±1.12
	RndSVD	77.62±0.74	73.41±0.44	73.79±0.68	72.15±0.81	73.41±0.85	69.67±0.25	71.07±0.85
	Nyström	76.68±0.14	74.02±0.56	74.95±0.31	71.92±0.57	74.11±0.63	68.60±0.65	73.08±1.03

TABLE V

COMPARISON BETWEEN AT-GSE AND BASELINES ON CORA_ML. THE FIRST COLUMN (MODEL) AND THE SECOND COLUMN (AT, × MEANS MODELS WITHOUT AT) SHOW THE NAMES OF THE BASELINES AND OUR PROPOSED METHODS (LIGHT GRAY BACKGROUND) TOGETHER. GPRGNN AND APPNP IN THE LAST TWO LINES REPRESENT THE GNN MODELS; THESE ROWS ARE GPRGNN AND APPNP, RESPECTIVELY. THE SECOND LINE IS THE RATE OF BUDGET. THE BEST RESULT IS HIGHLIGHTED IN **BOLD**.

Model	AT	Clean	LRBCD	PRBCD	LRBCD	PRBCD	LRBCD	PRBCD
		0%	5%		10%		25%	
GCN	×	84.12±0.11	77.15±0.58	74.19±0.67	73.20±1.01	68.24±0.58	67.46±1.21	57.04±2.28
APPNP	×	82.29±0.23	80.67±1.11	74.33±0.79	77.85±1.00	67.89±1.33	73.10±1.10	56.90±1.68
GPRGNN	×	81.44±0.32	75.14±0.92	71.55±0.90	70.74±0.43	67.50±2.08	63.66±1.02	60.35±2.72
GCN	LRBCD	85.56±0.00	80.67±0.53	75.81±0.67	78.06±0.91	69.96±1.11	71.41±0.83	56.16±0.48
	PRBCD	85.49±0.21	79.30±0.56	76.51±0.52	76.23±0.96	70.00±1.02	70.46±1.26	57.43±0.91
APPNP	LRBCD	86.62±0.35	80.67±0.69	77.89±0.74	78.27±0.88	72.68±0.82	74.58±0.90	62.61±0.70
	PRBCD	85.11±1.32	79.65±1.54	78.94±0.44	77.89±1.23	73.10±0.87	73.38±1.32	61.37±0.61
GPRGNN	LRBCD	81.37±0.11	78.31±0.82	76.13±0.85	75.53±0.48	71.83±0.59	68.87±0.85	63.66±0.87
	PRBCD	81.02±0.56	77.15±1.93	76.13±0.34	73.45±1.26	71.41±0.26	67.61±1.32	62.43±0.52
GPRGNN	GSE	82.50±0.35	78.38±0.87	76.48±1.07	74.89±0.86	73.80±1.05	69.33±1.59	69.19±0.91
APPNP	RndSVD	87.75±0.14	81.37±0.68	78.42±0.45	78.94±0.70	72.71±0.50	74.89±0.83	60.67±0.89
GPRGNN	RndSVD	86.16±0.55	82.61±0.59	78.31±0.42	79.05±0.84	77.25±0.55	70.07±1.55	68.77±1.40
APPNP	Nyström	86.90±0.14	84.58±0.92	76.87±0.69	80.67±0.79	72.96±1.14	75.04±0.96	60.42±0.85
GPRGNN	Nyström	85.25±1.25	82.39±0.76	79.54±0.48	78.27±0.86	77.46±0.42	72.82±1.59	73.80±0.53

TABLE VI

COMPARISON BETWEEN AT-GSE AND BASELINES ON SBM(HOMO.). THE FIRST COLUMN (MODEL) AND THE SECOND COLUMN (AT, × MEANS MODELS WITHOUT AT) SHOW THE NAMES OF THE BASELINES AND OUR PROPOSED METHODS (LIGHT GRAY BACKGROUND) TOGETHER. GCN IN THE LAST LINE REPRESENTS THE BACKBONE GNN MODEL FOR AT-GSE. THE SECOND LINE IS THE RATE OF BUDGET. THE BEST MODEL IS HIGHLIGHTED IN **BOLD**.

Model	AT	Clean	LRBCD	PRBCD	LRBCD	PRBCD	LRBCD	PRBCD
		0%	5%		10%		25%	
GCN	×	86.46±0.49	80.20±0.49	80.61±0.76	77.47±0.91	78.48±1.57	63.74±0.71	70.81±1.31
APPNP	×	78.18±4.02	86.06±2.11	73.43±4.19	78.08±1.11	71.21±4.15	61.92±0.91	67.88±3.31
GPRGNN	×	65.15±8.81	52.12±2.60	63.84±8.04	51.92±2.13	63.43±7.98	51.11±1.03	62.53±7.52
GCN	LRBCD	86.77±0.30	81.72±0.54	84.14±0.65	79.39±0.49	82.83±1.20	68.59±0.84	80.30±0.51
	PRBCD	86.87±0.00	84.55±0.65	85.35±0.51	81.11±0.46	84.34±0.81	71.62±0.71	82.12±0.91
APPNP	LRBCD	86.26±3.70	81.72±1.15	79.60±2.38	76.06±1.57	76.67±2.84	62.83±0.99	70.71±1.69
	PRBCD	84.95±4.57	81.31±0.68	76.97±3.06	73.33±0.67	72.22±2.08	64.65±0.90	65.66±1.43
GPRGNN	LRBCD	82.53±0.46	80.81±0.00	78.48±2.17	78.08±0.46	76.97±2.01	72.53±0.88	73.94±2.20
	PRBCD	83.03±5.66	79.60±0.40	77.07±4.50	73.74±0.78	75.05±4.24	63.84±0.88	70.30±4.89
GCN	AT-GSE	88.89±0.00	84.95±0.30	86.06±0.61	81.72±0.30	85.25±0.67	70.00±1.02	83.13±0.65

TABLE VII

COMPARISON BETWEEN AT-GSE AND BASELINES ON SBM(HETERO.). THE FIRST COLUMN (MODEL) AND THE SECOND COLUMN (AT, × MEANS MODELS WITHOUT AT) SHOW THE NAMES OF THE BASELINES AND OUR PROPOSED METHODS (LIGHT GRAY BACKGROUND) TOGETHER. GPRGNN IN THE LAST LINE REPRESENTS THE BACKBONE GNN MODEL FOR AT-GSE. THE SECOND LINE IS THE RATE OF BUDGET. THE BEST RESULT IS HIGHLIGHTED IN **BOLD**.

Model	AT	Clean	LRBCD	PRBCD	LRBCD	PRBCD	LRBCD	PRBCD
		0%	5%		10%		25%	
GCN	×	62.63±1.01	60.61±1.01	60.30±0.65	58.69±1.05	60.10±0.81	53.54±1.69	56.97±1.70
APPNP	×	57.88±3.35	50.30±0.76	53.74±2.01	49.60±0.54	50.61±1.46	49.39±0.54	46.16±1.57
GPRGNN	×	61.52±8.59	59.60±11.43	61.01±8.05	59.26±11.03	61.01±8.05	56.87±8.02	59.70±6.71
GCN	LRBCD	61.62±0.00	59.19±0.49	60.40±0.88	57.98±0.49	59.19±1.37	53.64±0.30	56.16±1.64
	PRBCD	64.65±0.00	61.52±0.54	64.04±0.81	59.70±0.84	63.03±1.12	52.73±1.74	61.01±0.81
APPNP	LRBCD	49.49±0.00	49.49±0.00	49.49±0.00	49.49±0.00	49.49±0.00	49.49±0.00	49.49±0.00
	PRBCD	64.04±5.44	59.39±2.29	49.49±0.00	55.66±0.95	49.49±0.00	43.54±1.23	49.49±0.00
GPRGNN	LRBCD	82.73±1.39	82.63±1.34	79.49±1.87	75.96±0.76	71.72±5.21	65.66±3.94	68.79±4.05
	PRBCD	86.26±1.98	84.55±0.65	81.72±1.78	75.15±0.49	79.39±1.64	62.12±2.13	74.44±1.75
GPRGNN	AT-GSE	90.40±1.37	87.88±0.64	84.75±1.78	79.49±1.28	81.21±2.72	66.36±4.29	75.86±1.89

TABLE VIII

THE ORIGINAL MODEL AND AT-GSE ON CLEAN GRAPHS.

Model	AT	Cora	Cora_ML	Citeseer	SBM(homo.)	SBM(hetero.)
GCN	×	77.91±0.17	84.12±0.11	71.73±0.48	86.46±0.49	62.63±1.01
	AT-GSE	77.95±0.61	86.13±0.92	74.35±0.74	88.89±0.00	64.85±1.48
APPNP	×	79.05±1.06	85.53±0.87	70.98±1.30	78.18±4.02	57.88±3.35
	AT-GSE	82.64±0.18	87.75±0.14	73.13±0.60	80.51±4.50	60.61±2.78
GPRGNN	×	80.40±2.11	81.44±0.32	63.55±1.40	65.15±8.81	61.52±8.59
	AT-GSE	83.41±0.43	83.27±0.36	76.54±0.75	86.57±2.22	90.40±1.37

applicable to various types of graph data. However, existing studies reveal that adversarial training is difficult to be applied to large-scale graphs. What’s worse is that AT-GSE deals with singular value distribution, which may further impose the computational burden and prevent it from the potential applications to larger graph datasets. To resolve this issue, we propose two variants (RndSVD and Nyström) of AT-GSE models to improve the model’s training and classifying capabilities on larger-scale graph data.

As described in Section III-D1, RndSVD leverages random projection of the original large-sized adjacency matrix onto a low-dimensional subspace so as to reduce the computational complexity of SVD operations. The Nyström method is to calculate a low-rank approximation of the original adjacency matrix, avoiding the need of SVD operations (see

Section III-D2 for details). Both methods have theoretical guarantee of the approximation accuracy with substantially reduced computational complexity.

To demonstrate their practical usefulness, we randomly generated an adjacency matrix of a graph with 1,000 nodes to calculate the running time taken by the original SVD, RndSVD, and Nyström for every epoch. Experimental results show that SVD takes 3.9 seconds per epoch, RndSVD needs 0.1 seconds, and Nyström only consumes 0.05 seconds. It appears that **the running time of RndSVD and Nyström methods are nearly 40 times and 80 times faster than the vanilla SVD respectively**. In addition, we directly select the fastest method to test on the Pubmed dataset with about 20,000 nodes, which will be out-of-memory when running the original AT-GSE on a 40G GPU. The test outcomes are recorded in Table IX. Also

TABLE IX

COMPARISON BETWEEN AT-GSE WITH NYSTRÖM AND BASELINES ON PUBMED. THE FIRST COLUMN (MODEL) AND THE SECOND COLUMN (AT, × MEANS MODELS WITHOUT AT) SHOW THE NAMES OF THE BASELINES AND OUR PROPOSED METHODS (LIGHT GRAY BACKGROUND) TOGETHER. GPRGNN IN THE LAST LINE REPRESENTS THE BACKBONE GNN MODEL FOR AT-GSE. THE SECOND LINE IS THE ATTACK RATIO. THE BEST RESULT IS HIGHLIGHTED IN BOLD.

Model	AT	Clean	LRBCD	PRBCD	LRBCD	PRBCD	LRBCD	PRBCD
		0%	5%		10%		25%	
GCN	×	72.45±0.06	67.29±0.15	69.19±0.25	65.54±0.24	61.56±0.16	62.00±0.34	47.30±0.60
APPNP	×	74.45±0.10	69.35±0.23	71.91±0.17	67.71±0.26	65.72±0.29	63.61±0.33	53.61±0.42
GPRGNN	×	74.50±0.90	70.72±0.90	73.60±0.48	68.16±0.73	69.94±0.90	63.64±0.98	64.71±1.54
GCN	LRBCD	76.06±0.08	70.81±0.17	70.73±0.26	69.03±0.37	63.19±0.36	65.53±0.34	49.22±0.53
	PRBCD	72.48±0.00	68.19±0.21	70.15±0.24	66.62±0.19	63.43±0.27	63.21±0.34	49.45±0.52
APPNP	LRBCD	72.70±0.10	69.59±0.26	69.22±0.25	68.10±0.19	64.76±0.43	64.97±0.21	54.92±0.33
	PRBCD	77.54±0.39	72.87±0.22	73.45±0.34	70.28±0.42	68.46±0.27	66.15±0.41	57.97±0.36
GPRGNN	LRBCD	75.62±0.27	72.73±0.35	71.32±0.34	71.48±0.25	68.10±0.26	69.32±0.16	62.46±0.50
	PRBCD	75.72±0.31	73.22±0.52	74.14±0.23	71.06±0.68	70.52±0.44	68.24±0.83	64.48±0.46
GPRGNN	Nyström	79.22±0.00	75.43±0.16	74.24±0.17	72.70±0.21	70.94±0.35	69.26±0.11	66.27±0.14

using the 40G GPU, Nyström can train the classify prediction results, most of which are better than our baselines. It is evident that **our proposed variants take up less storage space and also have great robustness on large-scale datasets.**

After determining the computational efficiency of AT-GSE with RndSVD and Nyström, we need to further verify that they also have excellent robust performance. Therefore, we compared these two methods of AT-GSE with baselines on the Cora, Citeseer and Cora_ML datasets too. The results are also shown in Table III, Table IV and Table V. These two variants substantially reduce time complexity at the cost of slightly degraded robustness performance. **It is worth noting that they have almost the same performances as the original AT-GSE.** Specifically, the prediction accuracy of AT-GSE using RndSVD or Nyström is greater than that of baselines, indicating that they are end up with more robust GNN models. The strongest effect based on different backbone models shows that they are also selective to different backbone models. Moreover, the applicability to different datasets reflects good generalization ability. In other words, these two AT-GSE methods, especially Nyström, yield excellent robustness, generalization, and scalability performance, and can be a promising candidate of robust GNN training methods.

More interestingly, AT-GSE with RndSVD and Nyström exhibits different behaviors in defending against local and global topology attacks. According to the comparison of these two methods, we can find that RndSVD is more dedicated to the local graph properties compared to Nyström. It retains all graph properties related to the low-rank parts, discards unnecessary high-rank parts, and only adjusts the medium-parts that are most vulnerable to topology attacks. In contrast, the Nyström method is of high simplicity without time-consuming SVD operations. It modifies the graph’s global properties by adjusting the low-rank/low-frequency graph spectrum as a whole. Therefore, when they are applied to AT-GSE, **RndSVD is expected to defend local attacks, while Nyström is more favorable global attacks.** Evidently, in Figure 4, Figure 5, and Figure 6, for local LRBCD attacks, SVD or RndSVD is better, while Nyström performs better against global PRBCD attacks.

Finally, we also tested the prediction results of AT-GSE with

Nyström on the larger heterophily graph, e.g., the WikiCS dataset. Table X shows that the AT-GSE-like method that reduces computational complexity also shows **its strong robust performance for heterophily graphs**, outperforming the existing state-of-the-art methods.

To conclude, by leveraging graph subspace energy as a regularizer in the adversarial training of GNN models on inductive learning, AT-GSE possesses excellent robustness, generalization, and scalability performance and should be of practical significance.

V. CONCLUSION

We proposed an adversarial training with graph subspace energy (AT-GSE) method to improve GNN robustness to adversarial perturbations in the node classification task on inductive learning. Our proposed AT-GSE method improves GNN adversarial robustness by protecting the singular value distribution of the adjacency matrix, which is vulnerable to adversarial topology attacks in the inference phase. It turns out that GSE is a reasonable measurable indicator of GNN robustness and a suited control of GSE could yield more robust GNN models. We also proposed AT-GSE with RndSVD and Nyström approximation to defend against the local and global topology perturbations respectively, with enhanced computational efficiency. Extensive experiments conducted on 7 datasets in an inductive learning setting demonstrate the superiority of our proposed AT-GSE method in robustness, generalization, and scalability to the state-of-the-art methods. Theoretical underpinnings of GSE towards GNN adversarial robustness and the scalability to larger-sized graph datasets are interesting yet challenging open questions for future works.

REFERENCES

- [1] Y. Wu, D. Lian, Y. Xu, L. Wu, and E. Chen, “Graph convolutional networks with markov random field reasoning for social spammer detection,” in *Proceedings of the AAAI conference on artificial intelligence*, 2020, pp. 1054–1061.
- [2] A. Sanchez-Gonzalez, N. Heess, J. T. Springenberg, J. Merel, M. Riedmiller, R. Hadsell, and P. Battaglia, “Graph networks as learnable physics engines for inference and control,” in *International conference on machine learning*. PMLR, 2018, pp. 4470–4479.

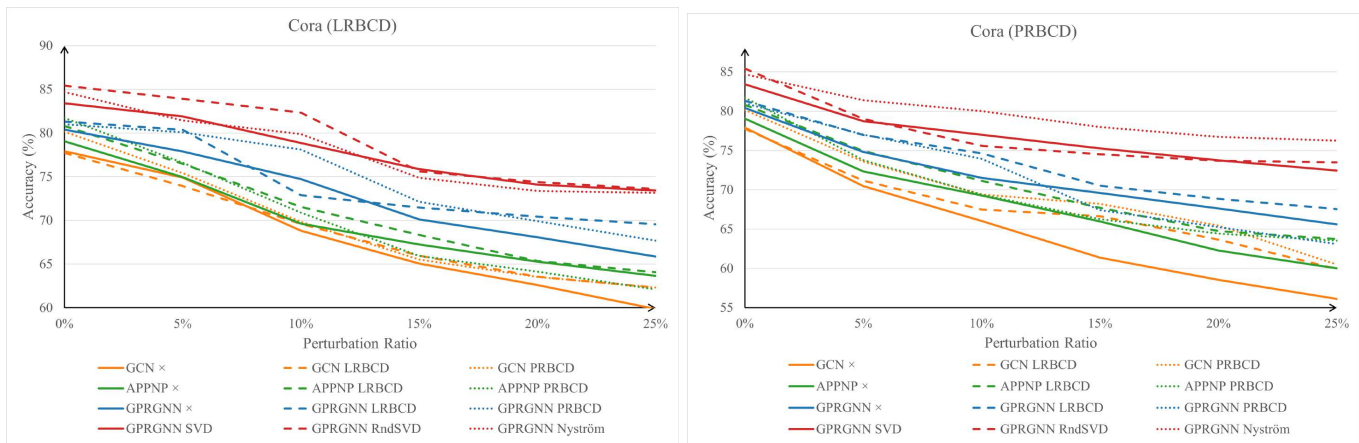


Fig. 4. The accuracy of each model on the Cora dataset under LRBCD (left) or PRBCD (right) attacks. In the legend, the former is the backbone model and the latter is the name of the method for generating adversarial examples. For example, GPRGNN RndSVD is an adversarial training with GPRGNN as the backbone model and RndSVD generating adversarial examples. The red line in the figure is the method we proposed, and the rest are baselines.

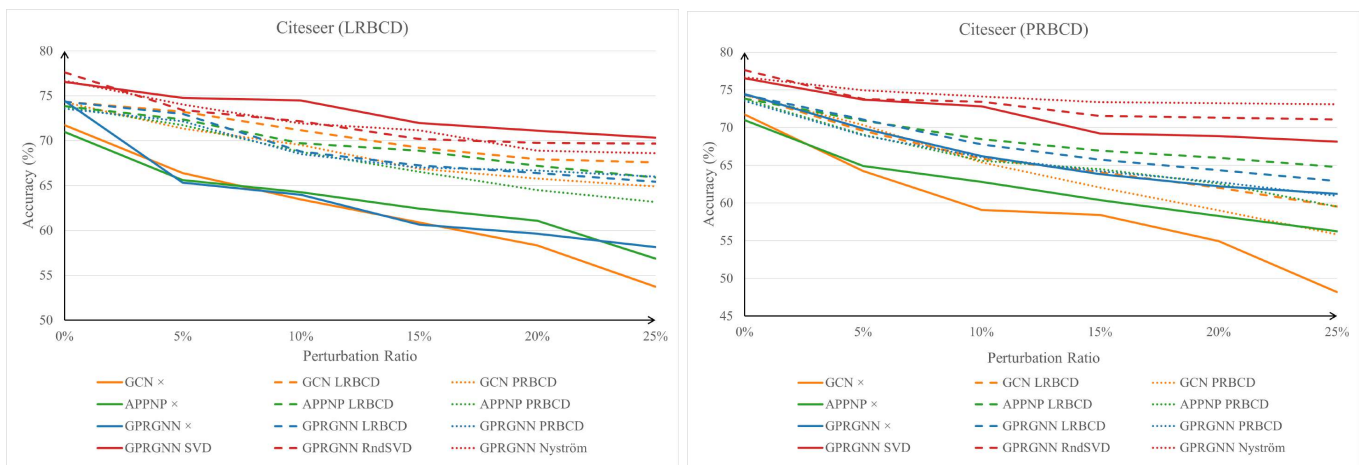


Fig. 5. The accuracy of each model on the Citeseer dataset under LRBCD (left) or PRBCD (right) attacks. In the legend, the former is the backbone model and the latter is the name of the method for generating adversarial examples. For example, GPRGNN RndSVD is an adversarial training with GPRGNN as the backbone model and RndSVD generating adversarial examples. The red line in the figure is the method we proposed, and the rest are baselines.

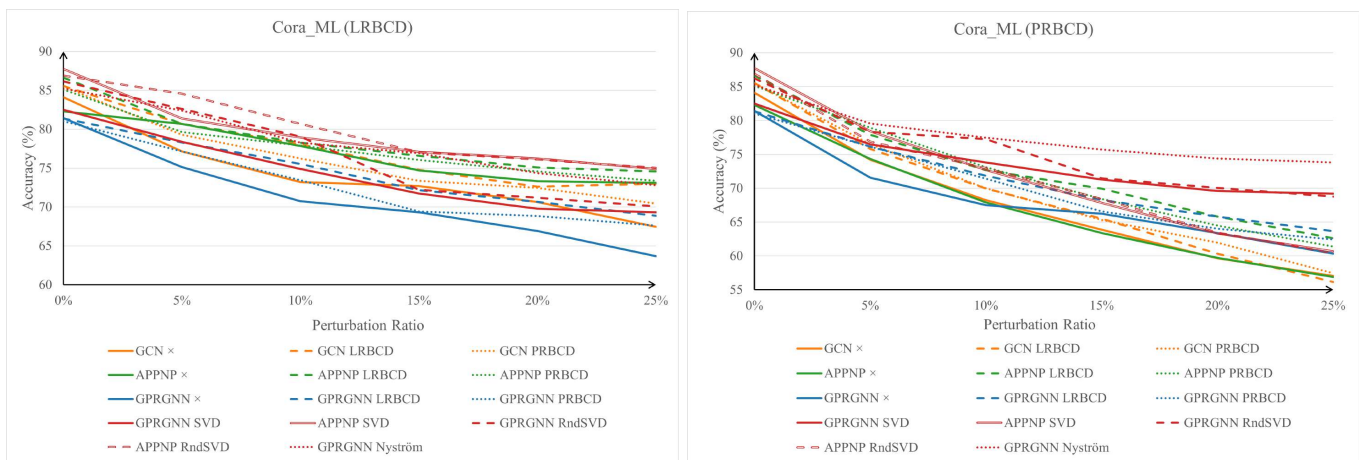


Fig. 6. The accuracy of each model on the Cora dataset under LRBCD (left) or PRBCD (right) attacks. In the legend, the former is the backbone model and the latter is the name of the method for generating adversarial examples. For example, GPRGNN RndSVD is an adversarial training with GPRGNN as the backbone model and RndSVD generating adversarial examples. The red line in the figure is the method we proposed, and the rest are baselines.

TABLE X

COMPARISON BETWEEN AT-GSE WITH NYSTRÖM AND BASELINES ON WIKICS. THE FIRST COLUMN (MODEL) AND THE SECOND COLUMN (AT, × MEANS MODELS WITHOUT AT) SHOW THE NAMES OF THE BASELINES AND OUR PROPOSED METHODS (LIGHT GRAY BACKGROUND) TOGETHER. GPRGNN IN THE LAST LINE REPRESENTS THE BACKBONE GNN MODEL FOR AT-GSE. THE SECOND LINE IS THE ATTACK RATIO. THE BEST RESULT IS HIGHLIGHTED IN BOLD.

Model	AT	Clean	LRBCD	PRBCD	LRBCD	PRBCD	LRBCD	PRBCD
		0%	5%		10%		25%	
GCN	×	73.13±0.00	50.75±0.47	51.07±0.34	44.86±0.50	45.29±0.43	39.85±0.35	36.85±0.26
APPNP	×	73.00±1.11	59.06±1.45	56.72±0.91	55.00±1.84	51.31±0.73	48.33±1.41	43.44±1.23
GPRGNN	×	72.69±0.00	60.33±0.41	62.17±0.64	57.03±0.24	58.41±0.34	53.07±0.39	53.14±0.50
GCN	LRBCD	76.22±0.44	63.52±0.68	59.82±0.27	60.12±0.49	53.84±0.32	56.56±0.47	44.51±0.47
	PRBCD	75.90±0.61	59.70±0.73	57.97±0.37	55.01±0.45	51.81±0.50	51.04±0.50	42.48±0.40
APPNP	LRBCD	75.39±0.24	65.63±0.59	64.78±0.34	62.24±0.42	60.54±0.34	58.43±0.54	52.71±0.52
	PRBCD	75.99±0.41	63.77±0.56	62.29±0.79	60.63±0.74	57.54±0.50	56.09±0.89	50.33±0.51
GPRGNN	LRBCD	73.92±0.51	64.43±0.67	67.42±0.51	63.14±0.91	66.05±0.54	61.91±0.67	63.36±0.60
	PRBCD	76.04±0.67	66.84±0.73	68.00±0.77	64.22±1.15	65.88±0.82	61.36±1.20	61.91±0.83
GPRGNN	Nyström	78.64±0.63	67.58±1.19	69.36±0.49	64.66±1.10	66.68±0.39	61.46±0.28	61.54±0.95

- [3] T. Hamaguchi, H. Oiwa, M. Shimbo, and Y. Matsumoto, “Knowledge transfer for out-of-knowledge-base entities: A graph neural network approach,” *arXiv preprint arXiv:1706.05674*, 2017.
- [4] E. Khalil, H. Dai, Y. Zhang, B. Dilkina, and L. Song, “Learning combinatorial optimization algorithms over graphs,” *Advances in neural information processing systems*, vol. 30, 2017.
- [5] T. N. Kipf and M. Welling, “Semi-supervised classification with graph convolutional networks,” in *International Conference on Learning Representations (ICLR)*, 2017.
- [6] M. Zhang, L. Hu, C. Shi, and X. Wang, “Adversarial label-flipping attack and defense for graph neural networks,” in *2020 IEEE International Conference on Data Mining (ICDM)*. IEEE, 2020, pp. 791–800.
- [7] G. Liu, X. Huang, and X. Yi, “Adversarial label poisoning attack on graph neural networks via label propagation,” in *European Conference on Computer Vision*. Springer, 2022, pp. 227–243.
- [8] D. Zügner and S. Günnemann, “Adversarial attacks on graph neural networks via meta learning,” in *International Conference on Learning Representations (ICLR)*, 2019.
- [9] D. Zügner, A. Akbarnejad, and S. Günnemann, “Adversarial attacks on neural networks for graph data,” in *Proceedings of the 24th ACM SIGKDD international conference on knowledge discovery & data mining*, 2018, pp. 2847–2856.
- [10] S. Geisler, T. Schmidt, H. Şirin, D. Zügner, A. Bojchevski, and S. Günnemann, “Robustness of graph neural networks at scale,” *Advances in Neural Information Processing Systems*, vol. 34, pp. 7637–7649, 2021.
- [11] L. Gosch, S. Geisler, D. Sturm, B. Charpentier, D. Zügner, and S. Günnemann, “Adversarial training for graph neural networks: Pitfalls, solutions, and new directions,” *Advances in Neural Information Processing Systems*, vol. 36, 2024.
- [12] H. Wu, C. Wang, Y. Tyshetskiy, A. Docherty, K. Lu, and L. Zhu, “Adversarial examples for graph data: deep insights into attack and defense,” in *Proceedings of the 28th International Joint Conference on Artificial Intelligence*, 2019, pp. 4816–4823.
- [13] N. Entezari, S. A. Al-Sayouri, A. Darvishzadeh, and E. E. Papalexakis, “All you need is low (rank) defending against adversarial attacks on graphs,” in *Proceedings of the 13th International Conference on Web Search and Data Mining*, 2020, pp. 169–177.
- [14] W. Jin, T. Derr, Y. Wang, Y. Ma, Z. Liu, and J. Tang, “Node similarity preserving graph convolutional networks,” in *Proceedings of the 14th ACM international conference on web search and data mining*, 2021, pp. 148–156.
- [15] W. Jin, Y. Ma, X. Liu, X. Tang, S. Wang, and J. Tang, “Graph structure learning for robust graph neural networks,” in *Proceedings of the 26th ACM SIGKDD international conference on knowledge discovery & data mining*, 2020, pp. 66–74.
- [16] K. Xu, H. Chen, S. Liu, P.-Y. Chen, T.-W. Weng, M. Hong, and X. Lin, “Topology attack and defense for graph neural networks: An optimization perspective,” *arXiv preprint arXiv:1906.04214*, 2019.
- [17] K. Xu, S. Liu, P.-Y. Chen, M. Sun, C. Ding, B. Kailkhura, and X. Lin, “Towards an efficient and general framework of robust training for graph neural networks,” in *ICASSP 2020-2020 IEEE International Conference on Acoustics, Speech and Signal Processing (ICASSP)*. IEEE, 2020, pp. 8479–8483.
- [18] Z. Deng, Y. Dong, and J. Zhu, “Batch virtual adversarial training for graph convolutional networks,” *AI Open*, vol. 4, pp. 73–79, 2023.
- [19] F. Feng, X. He, J. Tang, and T.-S. Chua, “Graph adversarial training: Dynamically regularizing based on graph structure,” *IEEE Transactions on Knowledge and Data Engineering*, vol. 33, no. 6, pp. 2493–2504, 2019.
- [20] H. Jin and X. Zhang, “Latent adversarial training of graph convolution networks,” in *ICML workshop on learning and reasoning with graph-structured representations*, vol. 2, 2019.
- [21] J. Chen, X. Lin, H. Xiong, Y. Wu, H. Zheng, and Q. Xuan, “Smoothing adversarial training for gnn,” *IEEE Transactions on Computational Social Systems*, vol. 8, no. 3, pp. 618–629, 2020.
- [22] J. Li, J. Peng, L. Chen, Z. Zheng, T. Liang, and Q. Ling, “Spectral adversarial training for robust graph neural network,” *IEEE Transactions on Knowledge and Data Engineering*, 2022.
- [23] J. Guo, S. Li, Y. Zhao, and Y. Zhang, “Learning robust representation through graph adversarial contrastive learning,” in *International Conference on Database Systems for Advanced Applications*. Springer, 2022, pp. 682–697.
- [24] D. Zhu, Z. Zhang, P. Cui, and W. Zhu, “Robust graph convolutional networks against adversarial attacks,” in *Proceedings of the 25th ACM SIGKDD international conference on knowledge discovery & data mining*, 2019, pp. 1399–1407.
- [25] P. Drineas and M. W. Mahoney, “On the nyström method for approximating a gram matrix for improved kernel-based learning,” *Journal of Machine Learning Research*, vol. 6, no. Dec, pp. 2153–2175, 2005.
- [26] E. Richard, P.-A. Savalle, and N. Vayatis, “Estimation of simultaneously sparse and low rank matrices,” in *Proceedings of the 29th International Conference on Machine Learning*, 2012, pp. 51–58.
- [27] N. Halko, P.-G. Martinsson, and J. A. Tropp, “Finding structure with randomness: Probabilistic algorithms for constructing approximate matrix decompositions,” *SIAM review*, vol. 53, no. 2, pp. 217–288, 2011.
- [28] P. Sen, G. Namata, M. Bilgic, L. Getoor, B. Galligher, and T. Eliassi-Rad, “Collective classification in network data,” *AI magazine*, vol. 29, no. 3, pp. 93–93, 2008.
- [29] G. Namata, B. London, L. Getoor, B. Huang, and U. EDU, “Query-driven active surveying for collective classification,” in *10th International Workshop on Mining and Learning with Graphs*, vol. 8, 2012, p. 1.
- [30] Y. Deshpande, S. Sen, A. Montanari, and E. Mossel, “Contextual stochastic block models,” *Advances in Neural Information Processing Systems*, vol. 31, 2018.
- [31] J. Klicpera, A. Bojchevski, and S. Günnemann, “Predict then propagate: Graph neural networks meet personalized pagerank,” in *International Conference on Learning Representations, ICLR, 2019*, 2019.
- [32] E. Chien, J. Peng, P. Li, and O. Milenkovic, “Adaptive universal generalized pagerank graph neural network,” in *International Conference on Learning Representations*, 2020.